

In situ forming degradable networks and their application in tissue engineering and drug delivery

Kristi S. Anseth^{a,b,*}, Andrew T. Metters^a, Stephanie J. Bryant^a, Penny J. Martens^a, Jennifer H. Elisseff^c, Christopher N. Bowman^a

^aEngineering Center, Room ECCH 111, Department of Chemical Engineering, University of Colorado, Boulder, CO 80309-0424, USA

^bHoward Hughes Medical Institute, University of Colorado, Boulder, CO 80309-0424, USA

^cDivision of Intramural Research, National Institutes of Health, Bethesda, MD 20892-4370, USA

Received 20 February 2001; accepted 22 May 2001

Abstract

Multifunctional macromers based on poly(ethylene glycol) and poly(vinyl alcohol) were photopolymerized to form degradable hydrogel networks. The degradation behavior of the highly swollen gels was characterized by monitoring changes in their mass loss, degree of swelling, and compressive modulus. Experimental results show that the modulus decreases exponentially with time, while the volumetric swelling ratio increases exponentially. A degradation mechanism assuming pseudo first-order hydrolysis kinetics and accounting for the structure of the crosslinked networks successfully predicted the experimentally observed trends in these properties with degradation. Once verified, the proposed degradation mechanism was extended to correlate network degradation kinetics, and subsequent changes in network structure, with release behavior of bioactive molecules from these dynamic systems. A theoretical model utilizing a statistical approach to predict the cleavage of crosslinks within the network was used to predict the complex erosion profiles produced by these hydrogels. Finally, the application of these macromers as in situ forming hydrogel constructs for cartilage tissue engineering is demonstrated. © 2002 Elsevier Science B.V. All rights reserved.

Keywords: Photopolymerization; Hydrogels; Degradation; Cartilage tissue engineering

1. Introduction

Numerous medical applications benefit from the ability to fabricate polymers in situ. For example, as an alternative to mercury amalgam fillings, ceramic

filled dimethacrylate monomers are photopolymerized with blue light to produce tooth colored restorations in situ [1]. Bone cements based on methyl methacrylate are redox or thermally cured in vivo to form rigid polymers to secure metallic orthopedic implants [2]. Hubbell et al. [3] presented some of the first work using *degradable* polymers that were photocured in vivo to prevent post-operative adhesions. The advantages of in situ polymerization are many. First, because the initial materials are often liquid solutions or moldable putties, the systems are

*Corresponding author. Present address: Engineering Center, Room ECCH 111, Department of Chemical Engineering, Campus Box 424, University of Colorado, Boulder, CO 80309-0424, USA. Tel.: +1-303-492-3147; fax: +1-303-735-0095.

E-mail address: kristi.anseth@colorado.edu (K.S. Anseth).

easily placed in complex shapes (e.g. tooth caries) and subsequently reacted to form a polymer of exactly the required dimensions. Second, the adhesion of the polymer to surrounding tissue is generally significantly improved because of intimate contact of the polymer with the tissue during formation and the resulting mechanical interlocking that can arise from surface microroughness. Third, the invasiveness of some surgical techniques is minimized as liquid solutions are easily introduced through needle injections and can be photocured with fiber optic cables using arthroscopic techniques.

In addition to these advantages, however, in situ polymerization also introduces many new challenges. Polymerization conditions for in vivo applications are quite adverse, including a narrow range of physiologically acceptable temperatures, requirement for nontoxic monomers and/or solvents, moist and oxygen-rich environments, the need for rapid processing and clinically suitable rates of polymerization. Photoinitiated polymerizations overcome many of these limitations since the initiation does not require elevated temperatures, and the polymerization rate is sufficiently rapid, occurring over a time period of a few seconds to several minutes, which allows the system to overcome oxygen inhibition and moisture effects.

Our research group has been particularly interested in the development and use of multifunctional monomers that can be photopolymerized to form crosslinked, *degradable* networks. Such materials provide advantages for numerous biological and medical applications, and when combined with photoinitiated polymerization, networks can be formed in situ under physiological conditions with temporal and spatial control of the polymerization process. In this area, our efforts have ranged from the design of multifunctional anhydride monomers that react to form highly crosslinked and surface eroding networks for fracture fixation applications [4,5] to high molecular weight macromers that produce loosely crosslinked and bulk degrading hydrogels for cartilage tissue engineering and drug delivery [6–8]. This manuscript presents both experimental and modeling results related to characterization of degradation behavior, macroscopic properties, and solute release from photocrosslinked hydrogels formed from multifunctional and degradable macromers. In addition,

the application of these hydrogels as in situ forming constructs for cartilage tissue engineering is demonstrated.

2. Materials and methods

2.1. Macromers

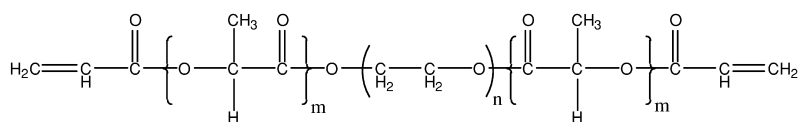
Multifunctional, degradable, and photocrosslinkable macromers based on poly(lactic acid) (PLA) and poly(ethylene glycol) (PEG) or poly(vinyl alcohol) (PVA) were synthesized according to the techniques and procedures first described by Sawhney et al. [9]. For example, triblock copolymers of PLA-b-PEG-b-PLA were synthesized and end-capped with acrylate functionalities, and graft copolymers of PLA-g-PVA were synthesized with methacrylate functionalities (Fig. 1). The multifunctionality of the macromers allowed photoinitiated polymerization and crosslinking of the macromer chains.

2.2. Hydrogel formation

For network characterization studies, photopolymerizations were initiated with 0.1 wt% Quantacure ITX photosensitizer (Biddle Sawyer) and Irgacure 907 (Ciba Geigy) and 15 mW/cm² of 420 nm light (Electro-Light). For controlled release experiments, photopolymerizations were initiated with 0.02 wt% Irgacure 651 (Ciba Geigy) and 15 mW/cm² of 365 nm light source (Blak-Ray; Model B100 AP). For cell encapsulation studies, previously determined cytocompatible initiation conditions were used [10]. The photoinitiating system was 0.05 wt% Darocur 2959 (Ciba Geigy) and a 365 nm initiating light source (Blak-Ray) at an intensity of ~8 mW/cm².

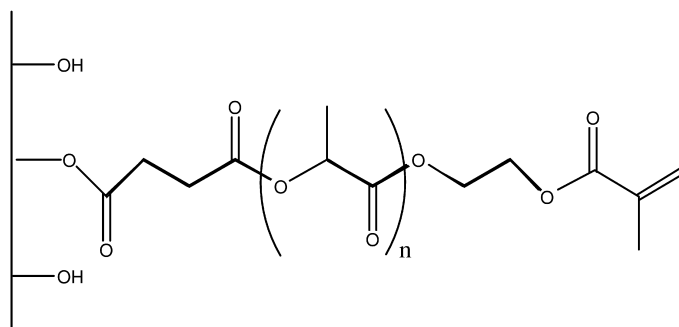
2.3. Network degradation characterization

Degradation of the photopolymerized hydrogels was carried out in a pH 7.4 phosphate-buffered saline solution (Fisher) at 37°C. At specified time points, disks were removed from the degradation medium; their swollen mass was measured in both air and heptane to obtain the swollen polymer volume; their static compressive modulus was then



PLA-b-PEG-b-PLA divinyl macromer

A



PLA-g-PVA multivinyl macromer

B

Fig. 1. Chemical structures of biodegradable, multifunctional, and photocrosslinkable macromers: (A) PLA-b-PEG-b-PLA macromer and (B) PLA-g-PVA macromer.

measured using a dynamic mechanical analyzer (Perkin Elmer) with a parallel plate configuration and a ramping stress of 400 mN/min; and their final mass was obtained after complete drying in a vacuum oven. From these measurements, the volume swelling ratio, compressive modulus, and mass loss were calculated as a function of degradation.

2.4. Release studies

Bovine serum albumin (BSA, Sigma) was photo-encapsulated in PLA-b-PEG-b-PLA based hydrogels. BSA was added to the macromer solution at concentrations up to 4.0 wt%, and photopolymerization of the final mixture produced hydrogel samples ~1 cm in diameter and 1 mm thick. Release behavior from hydrogels formed from two different macromers was examined. The first macromer had a PEG

core with an average molecular weight of 3400 Da, ~2.7 lactic acid repeat units flanking the PEG core, and 90% acrylation of the end groups. The second macromer had a PEG core with an average molecular weight of 2000 Da, ~2.2 lactic acid repeat units flanking the PEG core, and 70% acrylation of the end groups. To monitor BSA release as a function of hydrogel degradation, the gels were placed in vials containing a large excess (10 ml) of pH 7.4 phosphate buffered solution at 37°C. At specified time points, 0.5 ml samples of the vial buffer solution were taken and replaced by fresh buffer. After accounting for dilution caused by previous measurements, protein concentrations were measured with a Bio-Rad protein assay using the microassay procedure, in which a differential color change of the dye occurs in response to various protein concentrations. The color change was quantified by measur-

ing the absorbance at 596 nm with a UV–Vis spectrophotometer (Hewlett-Packard 8452A diode array).

2.5. Chondrocyte encapsulation

Chondrocytes were isolated from the femoral-patellar groove of a young calf (Research 87, Marlboro, MA) as described elsewhere [11]. The isolated chondrocytes were combined with the desired macromer/initiator solution and polymerized into a disk (~2 mm in thickness and ~6 mm in diameter) at a concentration of 100×10^6 cells/cm³. The constructs were cultured in non-treated tissue culture plates (12 well) using Dulbecco's Modified Eagle Medium (Gibco) supplemented with 1% penicillin-streptomycin (Gibco), 0.5 µg/ml fungizone (Gibco), 0.01 M MEM non-essential amino acids (Gibco), 10 mM Hepes, 0.04 mM l-proline, and 10% fetal bovine serum. The constructs were incubated at 37°C in a humid environment with 5% CO₂. Medium was replaced every 2–3 days.

2.5.1. Biochemical and histological analysis

The constructs were freeze dried for at least 48 h and then digested with a solution of 125 µg/ml papain type III (Worthington) and 10 mM l-cysteine (Aldrich) in PBE buffer (10 mM phosphate, 10 mM EDTA, pH 6.5). The polymer was crushed prior to digesting for 16 h at 60°C. Total glycosaminoglycan (GAG) content was determined using dimethylmethylene blue dye as described elsewhere [12]. For histological analysis, constructs were fixed in formalin and embedded in paraffin using standard histology procedures. Sections (~10 µm thick) were stained with Safranin O for glycosaminoglycans and counterstained with Fast Green.

2.5.2. Growth factor encapsulation

IGF-1 (100 µl of 10 µg IGF-1/ml stock, R&D Systems) and TGF-β (100 µl of 1 µg TGF-β/ml stock, R&D Systems) were encapsulated in 200 mg of poly(lactic acid-co-glycolic acid) (PLGA 50:50) microspheres using standard double emulsion techniques [13]. The IGF-1 stock solution was 10 mM acetic acid with 0.1% bovine serum albumin. The TGF-β stock solution was 4 mM HCl and 1 mg/ml

bovine serum albumin. The total protein loading of the IGF-1 and TGF-β microspheres was 15.0 ± 0.7 and 0.5 ± 0.1 ng/mg, respectively. A total of 15 mg of loaded microspheres were suspended and mixed in 1 ml of macromer/cell solution. The control groups included macromers and cells without microspheres and macromers and cells with unloaded microspheres. The suspensions were photopolymerized, incubated for 14 days, and biochemically analyzed [14].

3. Results and discussion

3.1. Network structure

Upon photopolymerization of the PEG and PVA based macromers, a three-dimensional degradable network is formed consisting of two distinct building blocks: (i) poly(meth)acrylate chains formed during the chain polymerization (i.e. kinetic chains) and (ii) PEG or PVA backbone segments from the macromer backbone forming the crosslinks or cycles. Fig. 2 illustrates this schematically for a divinyl or tetra-functional macromer (e.g. PEG-based macromers), but the network structure becomes exceedingly complex as the functionality of the macromer is increased. Multivinyl and degradable macromers are readily synthesized by increasing the degree of methacrylation on the PVA-based macromers, and these macromers lead to network structures with extensive cyclization, as well as multiple crosslinks per macromer.

In general, for the systems of interest, the vast majority of the network mass resides in the macromer backbone (i.e. the PEG or PVA segment). As with all hydrogels, the physical, mechanical, and transport properties of the gel are highly dependent on the backbone chemistry of the polymer, as well as the crosslinking density of the network. As degradation occurs, lactide ester linkages are cleaved homogeneously throughout the entire hydrogel at a rate controlled by the reaction kinetics for hydrolysis. This ongoing cleavage of crosslinks within the hydrogel systematically decreases the crosslinking density of the overall network.

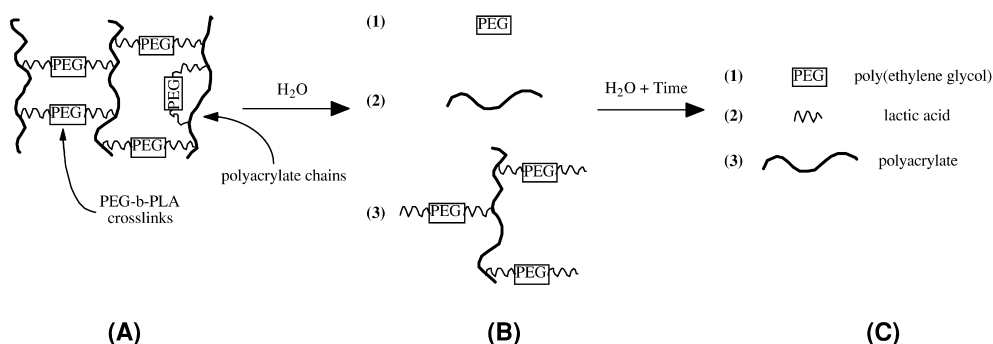


Fig. 2. Illustration of three different stages during the bulk degradation of a PLA-b-PEG-b-PLA hydrogel network: (A) initial and ideal, non-degraded PLA-b-PEG-b-PLA network, (B) primary erosion products that are released during degradation, and (C) final degradation products after complete hydrolysis.

3.2. Hydrogel degradation behavior

The degradation behavior of several photocrosslinked hydrogels was monitored through mass, swelling, and mechanical property measurements. Fig. 3 illustrates the typical *in vitro* degradation behavior for the compressive modulus (K) and volume swelling ratio (Q) as a function of degradation time. Immediately following polymerization, the hydrogel displays a high modulus and a low degree of swelling, indicative of a network with a relatively high degree of crosslinking. As degradation proceeds, the degradable PLA segments within the gel are hydrolyzed homogeneously, cleaving the network crosslinks. This process leads to a gel with a progressively lower crosslinking density, a

high degree of swelling, and an almost immeasurable compressive modulus.

As indicated by the fitted curves, the swelling of the hydrogel increases exponentially with a time constant, τ_Q , while the compressive modulus decays exponentially with a time constant τ_K . These experimentally observed exponential changes in the macroscopic gel properties with degradation can be explained by the justifiable assumption of a pseudo first order kinetic equation for hydrolysis of network crosslinks [15]. The first order hydrolysis kinetics equation is given by:

$$\frac{dn_E}{dt} = -k'_E n_E \quad (1)$$

where n_E represents the number of moles of degrad-

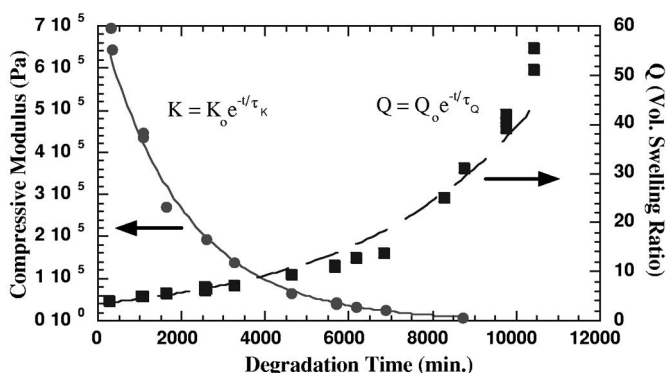


Fig. 3. Typical *in vitro* degradation behavior of a PLA-b-PEG-b-PLA hydrogel: compressive modulus (●) and volumetric swelling ratio (■). The solid and dashed lines are exponential curves fit to each property with time constants of $\tau_Q = 4200$ min and $\tau_K = 2000$ min.

able bonds (e.g. number of lactide ester bonds) and k'_E is the pseudo first order reaction rate constant for the hydrolysis of a single degradable linkage. This simplified kinetic expression assumes that the acid concentration, as well as the water concentration, is constant throughout the hydrogel degradation. In general, the molecular weight of the PLA degradable blocks on the macromers was low compared to the overall macromer molecular weight. Thus, the total concentration of acid groups in the gel during degradation is relatively low. In addition, all degradation experiments were conducted in a sink of phosphate buffered solution to maintain a constant pH of 7.4. Furthermore, the highly swollen nature of the gels lowers the concentration of acid species within the crosslinked networks even further while allowing for efficient removal of acidic degradation products. Finally, because of the high network swelling, the water concentration remains approximately constant throughout degradation.

Therefore, as the ester groups and crosslinks within these hydrogels are hydrolyzed and degradation proceeds, pseudo first order kinetics predict an exponential increase in the average molecular weight between crosslinks. For PLA-b-PEG-b-PLA divinyl macromers, the exponential change in the molecular weight between crosslinks (\overline{M}_c) is related to the physical and kinetic characteristics of the degrading hydrogel by:

$$\overline{M}_c \sim e^{2jk'_E t} \quad (2)$$

where j represents the number of lactide ester bonds per PLA block; t is the degradation time; and the factor of two arises because there are two PLA blocks per crosslink (Fig. 3), and the degradation of one or more ester bonds leads to the cleavage of a crosslink.

From a simplified form of the Flory-Rehner equation, the volumetric swelling ratio (Q) scales with \overline{M}_c to the 3/5th power when the gel is highly swollen (polymer volume fraction, $v_2 < 0.1$). Similarly, from rubber elasticity theory, the compressive modulus (K) scales with \overline{M}_c to the $-6/5$ th power for highly swollen gels. Thus, from first principles, the swelling ratio is predicted to increase exponentially with degradation time, and the compressive modulus is predicted to decrease exponentially with degradation time.

Furthermore, comparison of the time constants for the compressive modulus and swelling degradation curves reported in Fig. 3 indicates that the rate of modulus decay is approximately twice as fast as the rate at which swelling increases ($\tau_Q = -2\tau_K$). Again, these experimental results are supported through the commonly used thermodynamic relationships for non-degrading hydrogels, the Flory-Rehner equation and rubbery elasticity theory, to show that

$$K \sim Q^{-2} \quad (3)$$

While the results presented in Fig. 3, along with comparisons of the exponential time constants for the fitted data, illustrate good agreement between the macroscopic degradation studies and the fundamental thermodynamic equations, complexities arise during gel degradation that can not be completely described by the analysis presented here. These complexities result from assumptions in the analysis such as a relatively high degree of swelling and constant physical parameters, as well as non-idealities in the network structure. For an expanded discussion on these issues the reader is referred to Metters et al. [16,17].

3.3. Release behavior from degradable gels

Scaling laws developed to understand macroscopic gel properties with degradation were extended to understand and predict solute release behavior from these hydrogels. Specifically, the structural and transport characteristics of these degrading hydrogels that impact its application as a controlled release device were related to the crosslinking density of the networks and their hydrolytic degradation rate. Network mesh size and solute diffusivity in highly swollen degradable hydrogels are related through the average molecular weight between crosslinks (\overline{M}_c). As previously discussed, the Flory-Rehner equation for highly swollen gels simplifies to yield the relationship:

$$Q \sim (\overline{M}_c)^{3/5} \quad (4)$$

In addition, the mesh size of hydrogel networks (ξ) can be determined as described by Canal and Peppas [18]:

$$\xi = \nu_2^{1/3} (\overline{r_0^2})^{1/2} \quad (5)$$

where $(\overline{r_0^2})^{1/2}$ is the root-mean-squared end-to-end distance of the polymer chains in the unperturbed state, and ν_2 is the volume fraction of polymer in the swollen gel. Since $(\overline{r_0^2})^{1/2}$ is proportional to $\overline{M_c}$, a scaling relationship between the network mesh size and average molecular weight between crosslinks is given by:

$$\xi = Q^{1/3} (\overline{r_0^2})^{1/2} \sim (\overline{M_c})^{7/10} \quad (6)$$

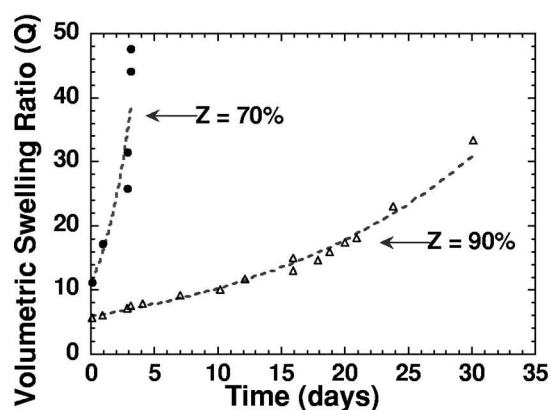
For homogeneous hydrogels, numerous equations and correlations exist to describe relationships between diffusivity and network structure. Here, a free volume approach developed by Lustig and Peppas [19] was chosen because of its proven accuracy and application in PEG-based hydrogels. Again, for high degrees of swelling ($\nu_2 < 0.1$),

$$\frac{D_g}{D_0} = \left(1 - \frac{r_s}{\xi}\right) \quad (7)$$

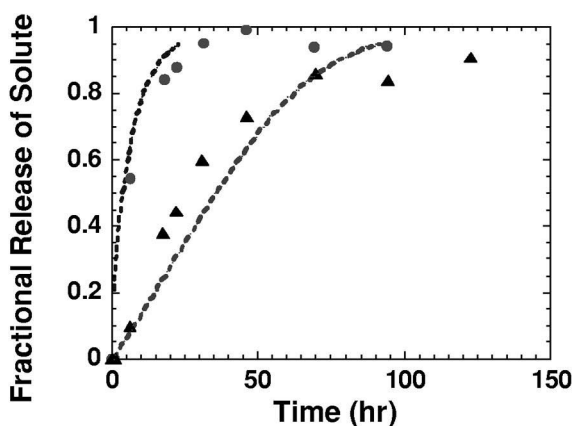
where D_g is the solute diffusivity in the swollen gel; D_0 is the solute diffusivity in the swelling solvent; and r_s is the radius of the solute. Combining Eqs. (6) and (7) gives the following scaling relationship between $\overline{M_c}$ and solute diffusion in highly swollen gels:

$$\left(1 - \frac{D_g}{D_0}\right) = \frac{r_s}{\xi} \sim (\overline{M_c})^{-7/10} \quad (8)$$

A number of experimental drug-release studies were performed to assess the suitability of the scaling laws to correlate drug-release to network degradation kinetics. In Fig. 4, the release of BSA was measured from two hydrogels synthesized from PLA-b-PEG-b-PLA macromers possessing different extents of acrylate functionalization of the macromer end groups (Z). As Z decreases, the initial cross-linking density decreases, thereby increasing the initial swelling ratio and mesh size, and the degradation rate dramatically increases (Fig. 4A). Both of these effects cause an overall increase in the drug release rate as seen in Fig. 4B. Predictions for the release behavior based on initial characteristics of the gels and their degradation kinetics are shown by the lines in Fig. 4B. The degradation-dependent function



A



B

Fig. 4. (A) Volumetric swelling ratio and (B) fractional release of BSA as a function of degradation time from two PLA-b-PEG-b-PLA hydrogels with varying extents of acrylate functionalization: (●) $Z = 70 \pm 5\%$ and (▲) $Z = 90 \pm 5\%$. Lines represent exponential fits to the swelling data (A) and solute release predictions based on scaling equations (B). $D_0 = 1.0 \times 10^{-5} \text{ mm}^2/\text{s}$ for both curves.

for the solute diffusion coefficient (Eq. (8)) was used to predict the solute release from the degrading hydrogel disk using the one-dimensional diffusional release equation for a uniformly loaded film [20]. In this case, the theoretical predictions match the experimental release profiles very well. The agreement between the theoretical and experimental results demonstrates that the scaling equations developed in this work are quite useful in relating the degradation properties of these hydrogels to solute release behavior.

3.4. Erosion behavior: experimental and modeling results

A statistical, mean-field model, based on fundamental parameters, was developed to predict and explain the complex erosion profile that occurs during the degradation of hydrogels formed from multifunctional macromers [21]. Mass loss from the photocrosslinked hydrogels is linked to network parameters such as the number of crosslinks per backbone chain and the mass fraction of the network contained in the backbone relative to the rest of the network. Model predictions versus degradation time also depend upon reaction parameters such as the order of the hydrolysis reaction and the value of the kinetic rate constant. Thus, the model accounts for both structural and kinetic issues.

In Fig. 5, experimental and predicted mass loss profiles are plotted versus degradation time for two PLA-b-PEG-b-PLA hydrogels polymerized in solution at different macromer concentrations. These degrading hydrogels have the same chemical composition, yet different initial crosslinking densities and microstructures that result from the polymerization behavior. Increasing the initial macromer concentration during polymerization increases the average kinetic chain length within the final network. This increase is reflected not only in an increased lag

time until reverse gelation occurs, but also a lower degradation rate constant, k'_E , due to the additional physical entanglements and the lower swelling ratios of these networks. These effects are clearly seen in Fig. 5. As the macromer concentration is increased from 25 to 50 wt%, k'_E decreases by $\sim 25\%$, resulting in the longer degradation time for the hydrogel produced from the 50 wt% macromer solution. The timescale for degradation of the second gel increases further due to an increase in the range of average kinetic chain lengths (L) from 35–50 repeat units to 130–170 repeat units per chain as predicted by the corresponding model fits.

Fig. 6 shows the dramatic influence of increasing the number of vinyl groups on the crosslinking molecules on the overall erosion behavior. For example, these results are indicative of differences observed in the mass loss profiles of networks synthesized from divinyl PEG-based macromers and multivinyl PVA-based macromers. As the number of vinyl groups on the crosslinking macromer increases, additional degradable units must be broken to release the crosslinker molecule. This effect results in longer inhibition times for the mass loss with increasing number of vinyl groups on the macromer. In addition, the fraction of the total network mass lost before the onset of reverse gelation (i.e. the divergence in the mass loss curve) decreases with an

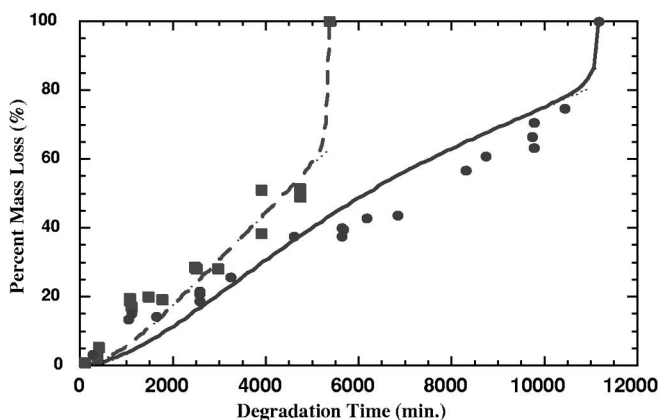


Fig. 5. Experimental mass loss data as a function of degradation time for hydrogels polymerized with varying macromer concentrations: (■) 25 wt% and (●) 50 wt%. The solid and dashed lines represent the percent mass loss predicted by a statistical model [6]: (dashed) 25 wt% and (solid) 50 wt%. Model parameters used for the hydrogels: (25 wt%) $k'_E = 5.0 \times 10^{-5} \text{ min}^{-1}$, $L = 35\text{--}50$; and (50 wt%) $k'_E = 3.8 \times 10^{-5} \text{ min}^{-1}$, $L = 130\text{--}170$. Other model parameters for both hydrogels: weight fraction PEG = 0.98, no cyclization, $Z = 82\%$, and 100% conversion.

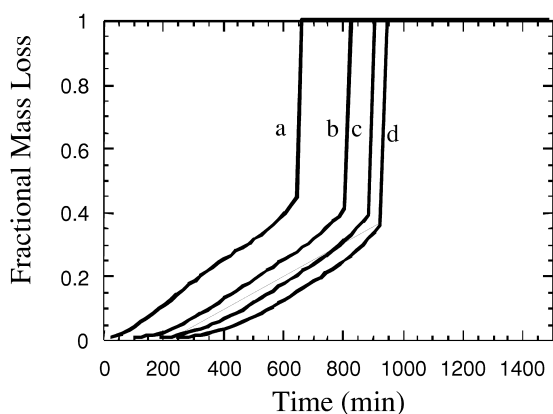


Fig. 6. Fractional mass loss as a function of degradation time for hydrogels with an increasing number of vinyl groups (m) on the crosslinking molecule: (a) $m=2$, (b) $m=4$, (c) $m=6$, and (d) $m=8$. Other model parameters: $L=100$, weight fraction in the crosslinking molecule=0.5, $k'_E=0.003 \text{ min}^{-1}$, 100% conversion, and no cyclization.

increase in the functionality of the macromer (i.e. a smaller amount of the network is released prior to reverse gelation).

3.5. *In situ* forming hydrogels for cartilage tissue engineering

These photocrosslinkable PEG and PVA-based macromers have been investigated for numerous applications including: *in situ* forming scaffolds for tissue engineering cartilage [6,7] and trans-tissue polymerized drug delivery implants and adhesives for seroma prevention [7,22]. Here, we illustrate the potential of these photocrosslinkable macromers to serve as scaffolds for tissue engineering cartilage. In tissue engineering cartilage, photopolymerization provides many benefits including rapid polymerization times under physiological conditions with temporal and spatial control over the polymerization. *In situ* forming hydrogels are attractive for their high water content and tissue-like elastic properties.

For cartilage tissue engineering applications, the idea of employing an *in situ* forming cell-hydrogel construct is that the polymer matrix serves temporarily as a replacement for the damaged cartilage until the cells lay down their own functional extracellular matrix. Since cartilage is comprised mainly of water, a high water content in the constructs is

desirable for transport of nutrients and waste through the gel. Ideally, the construct must also withstand the normal loads that native cartilage experiences. An advantage of these synthetic hydrogels is that they can easily be tailored to obtain a range of properties such as water content and compressive modulus. We have previously shown that by varying the percent macromer in solution the gel properties can be significantly varied [23]. However, in designing a successful matrix, a balance is required between high water content to maintain cell viability and good mechanics to withstand the loads of cartilage.

Studies were conducted to address several fundamental questions regarding the efficacy of photoencapsulating chondrocytes in *in situ* forming hydrogel networks and specifically: (i) the influence of the photopolymerization on cell viability; (ii) the composition of the neocartilage formed in these hydrogels *in vitro*; and (iii) the effects of properties associated with the hydrogel, such as transport, mechanics, and degradation, on the biochemical composition of the cartilage formed. Fig. 7 shows a histological section from chondrocytes that were photoencapsulated in a PEG-based hydrogel construct and stained with Safranin O to examine the glycosaminoglycan content (GAG). The histological evidence shows that chondrocytes remained healthy and produced GAG throughout the entire construct.

The biochemical content of the neocartilage formed in these photocrosslinked hydrogels was determined by quantifying the glycosaminoglycan (GAG) and total collagen contents at 4, 6, and 8 weeks *in vitro* to determine the cellular activity. Both the total collagen content and GAG content increased with time, indicating that the chondrocytes are metabolically active in these systems. At 8 weeks, the neocartilage was comprised of $0.4 \pm 0.09\%$ total collagen and $1.34 \pm 0.10\%$ GAG per wet weight of the construct, which is lower than that found in *in vivo* studies with photocrosslinked PEG macromers [7,14]. This result is likely related to the complex, *in vivo* environment where growth and other signaling factors are present. Thus, the ability to simultaneously photoencapsulate chondrocytes and growth factors in a single hydrogel matrix for cartilage tissue engineering would provide many advantages.

Results presented in Fig. 8 demonstrate the ability to enhance cartilage formation *in vitro* by encapsulat-

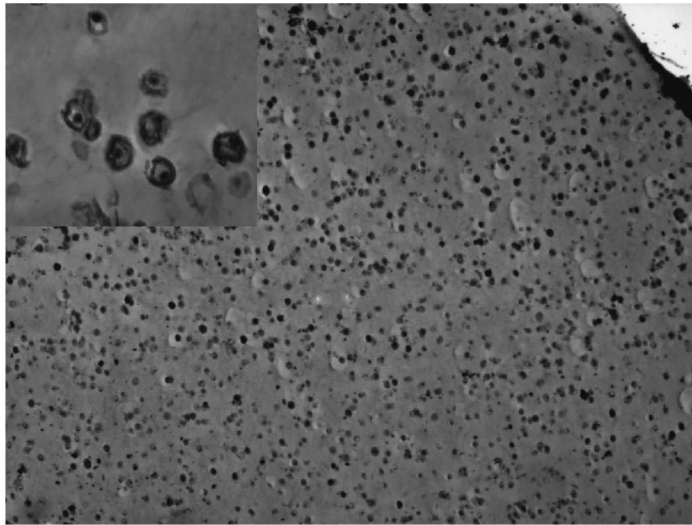


Fig. 7. Safranin O-stained histological section of neocartilage produced in a photocrosslinked PEG-based hydrogel after 6 weeks in vitro (40 \times). Inset picture is at 200 \times .

ing PLGA microspheres, loaded with insulin-like growth factor (IGF) and transforming growth factor-beta (TGF- β), in a photopolymerized hydrogel containing chondrocytes. IGF is synthesized locally

within chondrocytes and stored in the extracellular matrix (ECM). IGF interacts with other growth factors to mediate cell proliferation and ECM synthesis, and of particular interest here is the synergis-

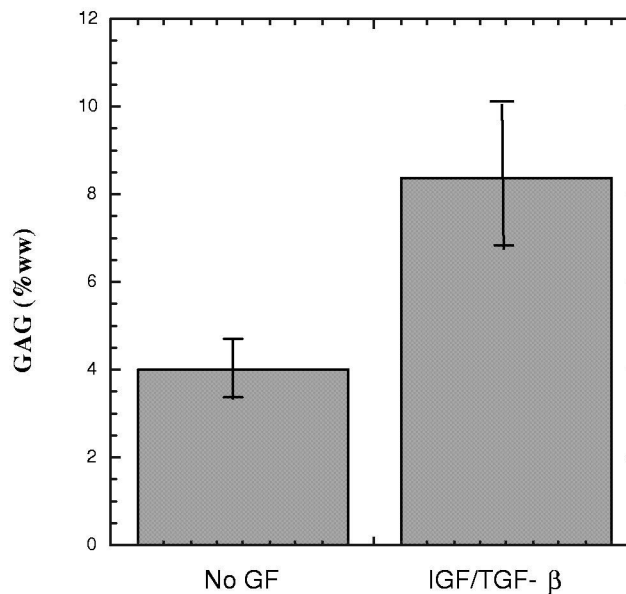


Fig. 8. In-vitro total GAG content per wet weight of the construct for chondrocytes encapsulated in photocrosslinked PEG-based hydrogels with and without growth factors after 14 days ($n=4$).

tic effects between IGF and TGF- β [24]. In cartilage, TGF- β inhibits cell proliferation and stimulates ECM production. The growth factors were encapsulated in PLGA microspheres to allow for a controlled and local delivery of the molecules in the hydrogels. Fig. 8 shows a significant increase in GAG production after 14 days in the constructs releasing IGF and TGF- β compared to the control (containing no growth factors). Over this time period, 55 ng/ml of IGF and 200 pg/ml of TGF- β were released from the microspheres. Conversely, since these low molecular weight growth factors can easily diffuse in the hydrogel matrix, IGF and TGF- β that was directly encapsulated in the hydrogel matrix without the microsphere carrier provided no benefit to ECM production over 14 days (data not shown).

Acknowledgements

The authors would like to acknowledge the support of this work from the National Institutes of Health (DE-12998), the Packard Foundation, and the Howard Hughes Medical Institute.

References

- [1] K. Anseth, S. Newman, C. Bowman, Polymeric dental composites: properties and reaction behavior of multi-methacrylate dental restorations, *Adv. Polym. Sci.* 122 (1995) 177–217.
- [2] D. Kohn, P. Ducheyne, in: R. Cahn, P. Haasen, E. Kramer (Eds.), *Medical and Dental Materials, Materials Science and Technology*, Vol. 14, VCH, New York, 1992, pp. 29–44.
- [3] J. Hill-West, S. Chowdhury, A. Sawhney, C. Pathak, R. Dunn, J. Hubbell, Prevention of postoperative adhesions in the rat by in situ photopolymerization of bioresorbable hydrogel barriers, *Obstet. Gynecol.* 83 (1994) 59–64.
- [4] K.S. Anseth, V.R. Shastri, R. Langer, Photopolymerizable degradable polyanhydrides, *Nat. Biotechnol.* 17 (1999) 156–159.
- [5] D. Svaldi Muggli, A.K. Burkoth, K.S. Anseth, Crosslinked polyanhydride networks for use in orthopaedic applications: degradation behavior and mechanics, *J. Biomed. Mater. Res.* 46 (1999) 271–278.
- [6] S.J. Bryant, K.S. Anseth, The effect of hydrogel thickness on tissue engineered cartilage in photocrosslinked poly(ethylene oxide) networks, *Biomaterials* 22 (2001) 619–626.
- [7] J.E. Elisseeff, K. Anseth, D. Sims, M. Randolph, R. Langer, Transdermal photopolymerizations for biomedical applications, *Proc. Natl. Acad. Sci. USA* 96 (1999) 3104–3107.
- [8] M.N. Mason, A.T. Metters, C.N. Bowman, K.S. Anseth, Predicting controlled-release behavior of degradable PLA-b-PEG-b-PLA hydrogels, *Macromolecules* 34 (2001) 4630–4635.
- [9] A.S. Sawhney, P.P. Chandrashekar, J.A. Hubbell, Bioerodible hydrogels based on photopolymerized poly(ethylene glycol)-co-poly(α -hydroxy acid) diacrylate monomers, *Macromolecules* 26 (1993) 581–587.
- [10] S.J. Bryant, C.R. Nuttelmen, K.S. Anseth, An evaluation of the cytocompatibility of several photoinitiating systems, *J. Biomater. Sci. Polym. Ed.* 11 (2000) 439–443.
- [11] L. Freed, G. Vunjak-Novakovic, in: J. Bronzind (Ed.), *The Biomedical Engineering Handbook*, 1995, pp. 1778–1796.
- [12] K.B. Taylor, G.M. Jeffree, A new basic methachromatic dye, I: 9-dimethyl methylene blue, *Histochem. J.* 1 (1969) 199–204.
- [13] S. Cohen, R. Yoshioka, R. Langer, Controlled delivery systems for proteins based on poly(lactic/glycolic acid) microspheres, *Pharm. Res.* 8 (1991) 713–720.
- [14] J.H. Elisseeff, *Transdermal Photopolymerization of Hydrogels for Tissue Engineering*, Ph.D. thesis (1999).
- [15] A.T. Metters, K.S. Anseth, C.N. Bowman, Fundamental studies of a novel, biodegradable PEG-b-PLA hydrogel, *Polymer* 41 (2000) 3993–4004.
- [16] A.T. Metters, C.N. Bowman, K.S. Anseth, Verification of scaling laws for degrading PLA-b-PEG-b-PLA hydrogels, *AIChE J.* 47 (2001) 1432–1437.
- [17] A.T. Metters, C.N. Bowman, K.S. Anseth, A statistical kinetic model for the bulk degradation of PLA-b-PEG-b-PLA hydrogel networks: incorporating network non-idealities, *J. Phys. Chem. B* 105 (2001) 8069–8076.
- [18] T. Canal, N.A. Peppas, Correlation between mesh size and equilibrium degree of swelling of polymeric networks, *J. Biomed. Mater. Res.* 23 (1989) 1183–1193.
- [19] S.R. Lustig, N.A. Peppas, Solute diffusion in swollen membranes. 9. Scaling laws for solute diffusion in gels, *J. Appl. Polym. Sci.* 36 (1988) 735–747.
- [20] J. Crank, *The Mathematics of Diffusion*, Clarendon Press, Oxford, 1975.
- [21] A.T. Metters, K.S. Anseth, C.N. Bowman, A statistical kinetic model for the bulk-degradation of PEG-b-PLA hydrogel networks, *J. Phys. Chem. B* 104 (2000) 7043–7049.
- [22] R.P. Silverman, J. Elisseeff, D. Passaretti, W. Huang, M.A. Randolph, M.J. Yaremchuk, Transdermal photopolymerized adhesive for seroma prevention, *Plast. Reconstr. Surg.* 103 (1999) 531–535.
- [23] P. Martens, K. Anseth, Characterization of hydrogels formed from acrylate modified poly(vinyl alcohol) macromers, *Polymer* 41 (2000) 7715–7722.
- [24] C.J. Malemud, The role of growth factors in cartilage metabolism, *Osteoarthritis* 19 (1993) 569–581.